LA-UR-01-0194
Approved for public release; distribution is unlimited.

Title:

Plasma Sprayed Functionally Graded and Layered $MoSi_2$-Al_2O_3 Composites for High Temperature Sensor Sheath Applications

Author(s):

Rajendra U. Vaidya, Richard G. Castro, David E. Gallegos, and John J. Petrovic

Submitted to:

Plasma Sprayed Functionally Graded and Layered $MoSi_2$-Al_2O_3 Composites for High Temperature Sensor Sheath Applications

Rajendra U. Vaidya, Richard G. Castro, David E. Gallegos, and John J. Petrovic

Los Alamos National Laboratory, Los Alamos, New Mexico, USA

Abstract

Protective sensor sheaths are required in the glass industry for sensors that are used to measure various properties of the melt. Molten glass presents an extremely corrosive elevated temperature environment, in which only a few types of materials can survive. Molybdenum disilicide ($MoSi_2$) has been shown to possess excellent corrosion resistance in molten glass, and is thus a candidate material for advanced sensor sheath applications. Plasma spray-forming techniques were developed to fabricate molybdenum dilicide-alumina (Al_2O_3) laminate and functionally graded composite tubes with mechanical properties suitable for sensor sheath applications. These functionally graded materials (FGMs) were achieved by manipulating the powder hoppers and plasma torch translation via in-house created computer software. Molybdenum disilicide and alumina are thermodynamically stable elevated temperature materials with closely matching thermal expansion coefficients. Proper tailoring of the microstructure of these $MoSi_2$-Al_2O_3 composites can result in improved strength, toughness, and thermal shock resistance. This study focuses on the mechanical performance of these composite microstructures.

1. Introduction

Advanced sensors for determining the properties of molten glass are a crucial need of the glass industry. Important processing parameters are molten glass temperature, viscosity, and chemistry. Molten glass is one of the most corrosive high temperature environments and hence sheaths made of materials that are corrosion resistant to molten glass must protect these sensors. The materials presently used for direct exposure in molten glass are noble metals such as platinum, refractory metals such as molybdenum, and refractory ceramics such as AZCS (alumina-zirconia-chromia-silica).

Thermocouple protection sheaths for thermocouples that are inserted into the molten glass through the air-glass line are presently either platinum tubes or platinum-coated Al_2O_3 tubes. Platinum is corrosion resistant above, at, and below the glass line. However, platinum is very expensive. Molybdenum tubes can be employed for thermocouples that traverse the glass line, but these must be extensively water-cooled, due to the poor oxidation resistance of molybdenum above the glass line. Molybdenum possesses good corrosion resistance to molten glasses when it is completely immersed in the molten glass. Refractory ceramics such as AZCS have good corrosion resistance to molten glass above, at, and below the glass line. However, dense AZCS ceramics are somewhat difficult to fabricate into long and narrow protective tubes. Furthermore, AZCS has very low strength and is susceptible to extensive plastic deformation at high temperatures.

Using platinum coatings on Al_2O_3 sheaths for thermocouples is the most commonly used practice in the glass industry. Protection of the thermocouple wires and Al_2O_3 sheathing is necessary to avoid corrosion and dissolution of the temperature-sensing unit. The cost associated with providing platinum coatings on the Al_2O_3 sheath material can be prohibitively high when taking into consideration the infrastructure needed at the glass plants to maintain and secure an inventory of available platinum. There are also issues associated with improving the performance of the platinum coated Al_2O_3. The failure rate of the thermocouples can be as high as 50%. The U.S. glass industry has been in search of alternative materials that can replace platinum and still provide the durability and performance needed to survive in an extremely corrosive glass environment.

Investigations by Park et al [1] have shown that $MoSi_2$ has comparable performance in molten glass as AZCS, Figure 1. The corrosion products and processes in the glass melt are identified in Figure 2. Molybdenum disilicide is a candidate high temperature material for such applications because of its high melting temperature (2030°C), relative low density (6.24g/cm^3), high thermal conductivity (52 W/mK), a brittle to ductile transition near 1000°C, and stability in a variety of corrosive and oxidative environments [2,3]. Additionally, the cost of $MoSi_2$ is significantly lower as compared to platinum coatings.

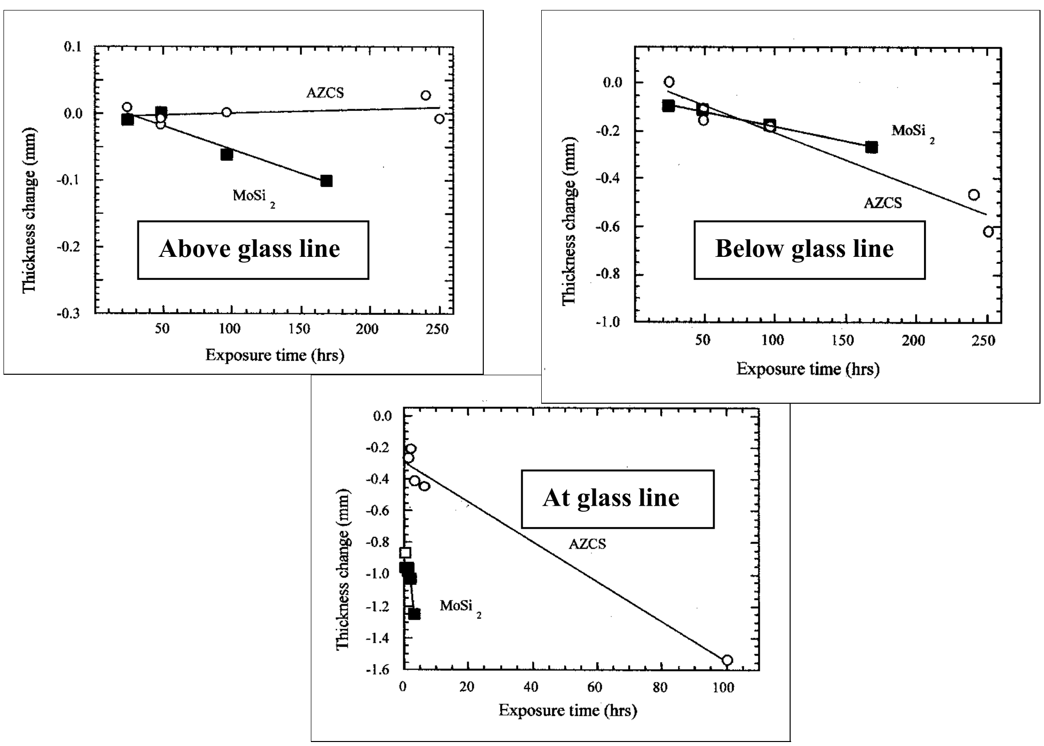

Figure 1. Comparative performance of AZCS and $MoSi_2$ in molten glass applications.

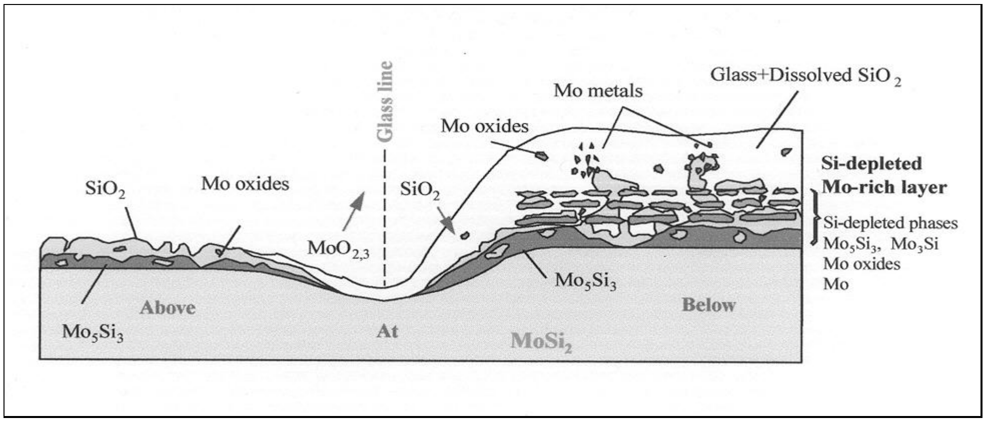

Figure 2. Corrosion products and processes involved during the immersion of $MoSi_2$ in molten glass.

Plasma spraying has been shown to be a very effective method for producing coatings and spray formed components of $MoSi_2$ and $MoSi_2$ composites [4]. Investigations on plasma spray formed layered $MoSi_2$-Al_2O_3 composite gas injection tubes were shown to have enhanced high temperature thermal shock resistance when immersed in molten copper and aluminum [5]. The composite tubes outperformed high-grade graphite and SiC tubes when immersed in molten copper and had similar performance to high-density graphite and mullite when immersed in molten aluminum. Energy absorbing mechanisms such as debonding (between the $MoSi_2$ and Al_2O_3 layers) and microcracking in the Al_2O_3 layer contributed to the composites' ability to absorb thermal stresses and strain energy during the performance test (shown in Figure 3). Furthermore, $MoSi_2$ and Al_2O_3 are chemically compatible and have similar thermal expansion coefficients [6,7].

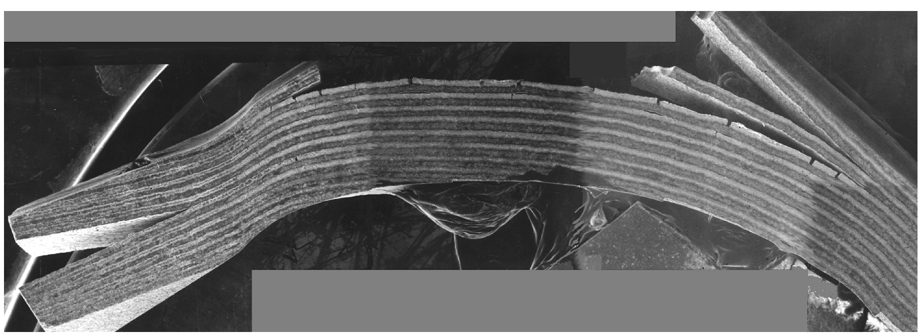

Figure 3. Four-point bend test beam after testing at 1400°C. Extensive debonding at the $MoSi_2$/Al_2O_3 interface and cracking within the Al_2O_3 was observed.

For thermocouple applications that require immersion of the thermocouple directly into molten glass, $MoSi_2$ coatings on Al_2O_3 protective sheaths need to be optimized. The thermocouple sheaths need to perform in both a high-temperature (>1300°C) oxidizing environment (above the glass line) and a highly corrosive molten glass environment (below the glass line). We are currently evaluating the potential use of a graded coating of Al_2O_3 to $MoSi_2$ to enhance the performance of the $MoSi_2$ in molten glass. The graded microstructure of the coating will reduce the residual stresses that can develop during the spray deposition process. These residual stresses can cause cracking and spallation of the coating. Preliminary results will be presented on the methodology used to produce the plasma sprayed $MoSi_2$-Al_2O_3 graded and layered composites and on the microstructure and mechanical behavior.

2. Experimental Procedures

Use of conventional plasma spraying equipment allows the flexibility of producing a variety of $MoSi_2$-Al_2O_3 microstructures, including laminate and graded structures. The plasma spraying equipment used for producing the composite microstructures included a Praxair Surface Technologies SG100 plasma torch and two Model 1264 powder feed hoppers. The plasma torch was mounted on a Fanuc S10 6-axis robot. A Technar DPV 2000 in-flight particle analyzer was used to measure the temperature, velocity and particle distribution of the $MoSi_2$ and Al_2O_3 particles as they exited the plasma torch. A computer control system was used to monitor and control the processing gases and the powder hoppers dispensing rate. Figure 4 shows an example of the computer control logic that was used to control the powder hopper rotation speed needed to produce the $MoSi_2$- Al_2O_3 continuously graded microstructure. In this figure, pure Al_2O_3 (Powder 2) is first deposited at a powder hopper rotation speed of 0.8 rpm. After an initial period of depositing pure Al_2O_3, $MoSi_2$ (Powder 1) is gradually introduced into the plasma torch by increasing the powder hopper rotational speed for $MoSi_2$ and decreasing the rotational speed for Al_2O_3. The powder hopper speed for $MoSi_2$ subsequently reaches 0.8 rpm and the Al_2O_3 powder dispensing speed goes to zero. Pure $MoSi_2$ is then deposited on the outside diameter of the tube. Argon was used for the plasma generating gas (40 standard liters per minute, slm) and as a carrier gas for the $MoSi_2$ and Al_2O_3 powders (1 to 4 slm). A Mikron TH 4104 infrared camera was used to measure and display the temperature of the substrate. POCO™ graphite tubes (12.7 mm OD, 9.5mm ID) were used as the substrates for the deposition runs.

The graded and layered $MoSi_2$-Al_2O_3 composites were fabricated by setting the powder hopper speeds and gas flow rates (to adjust the composition of the layers) prior to spraying. These rates were predetermined through preliminary experiments, and are shown in Table 1. Similar methodologies were employed in spraying the alternating layered samples. The thickness of the alternating $MoSi_2$ and Al_2O_3 layers were varied (0.07, 0.17, and 0.7 mm) in order to determine the optimum layer thickness.

To determine the mechanical behavior of the continuously graded and layered and graded $MoSi_2$-Al_2O_3 structures, C-rings were machined from the material deposited on the graphite tubes. C-ring samples were wire electro- discharge machined (EDM) out of the sprayed tube samples. The C-rings had an OD of 25.93 mm, an ID of 12.8 mm and a width of 10.76 mm. The critical $b/(r_o-r_i)$ ratio was 1.64, within the required range of 1 to 4. The C-ring samples were tested in diametrical compression using a hydraulic Instron test frame (Type 1331 with an 8500 Plus controller and a 10kN load cell), at a crosshead speed of 0.125 mm/min (strain rate ~ 0.316×10^{-4} s^{-1}). Machine compliance was corrected using a standard Al_2O_3 sample of known stiffness. All of the samples were machined and tested in accordance with ASTM Standard C 1323-96. Twelve samples for each composite tube were tested. Four samples of monolithic plasma sprayed $MoSi_2$ and Al_2O_3 were tested and used for comparison. A Weibull statistical approach was used to obtain the strength distributions in the coated and uncoated samples. While the standardized student-t test employing the normal or gaussian frequency distribution is often used in statistical analysis, there is no theoretical or experimental justification for using it in problems involving fracture. Use of a normal distribution is often inappropriate in analyzing fracture problems with plasma-sprayed ceramic materials because of the presence of multiple flaw populations. The Weibull distribution is more appropriate (and conservative) in this scenario because it does not require that the flaw population be normally distributed.

Table 1. Hopper speed and powder gas flow rates used in spraying the layered and graded sample.

Layer #	Al_2O_3 hopper speed (rpm)	Al_2O_3 gas flow rate (slm)	$MoSi_2$ hopper speed (rpm)	$MoSi_2$ gas flow rate (slm)	Spray time (sec)	Composition of layer
1 (Inner)	0.8	4.0	0	0	1600	100% Al_2O_3
2	0.8	4.0	0.3	2.0	1565	90% Al_2O_3,10% $MoSi_2$
3	0.8	4.0	0.5	2.0	1450	82% Al_2O_3,18% $MoSi_2$
4	0.8	4.0	0.5	4.0	1200	66% Al_2O_3,34% $MoSi_2$
5	0.8	4.0	0.8	4.0	925	49% Al_2O_3,51% $MoSi_2$
6	0.5	4.0	0.8	4.0	1065	31% Al_2O_3,69% $MoSi_2$
7	0.5	2.0	0.8	4.0	1325	13% Al_2O_3,87% $MoSi_2$
8	0.3	2.0	0.8	4.0	1465	6% Al_2O_3,94% $MoSi_2$
9 (Outer)	0	0	0.8	4.0	1510	100% $MoSi_2$

The mechanical strength of the layered samples was evaluated in four-point bending. Test samples 25mm long x 5mm wide x 2.5mm thick were electro-discharged (EDM) machined and surface ground using a 150 and 320 grit grinding wheel. Bending tests were performed in the above mentioned Instron machine using a cross-head speed of 0.125 mm/min (strain rate ~ 1.1×10^{-3} s^{-1}). The samples were tested in a self-aligning hardened steel fixture and were supported on steel pins 19 mm apart. Loading was accomplished by two steel pins 9.5 mm apart. The four-point bend tests were carried out in accordance with ASTM standard C-1161/90. Ten samples were tested for each layer thickness.

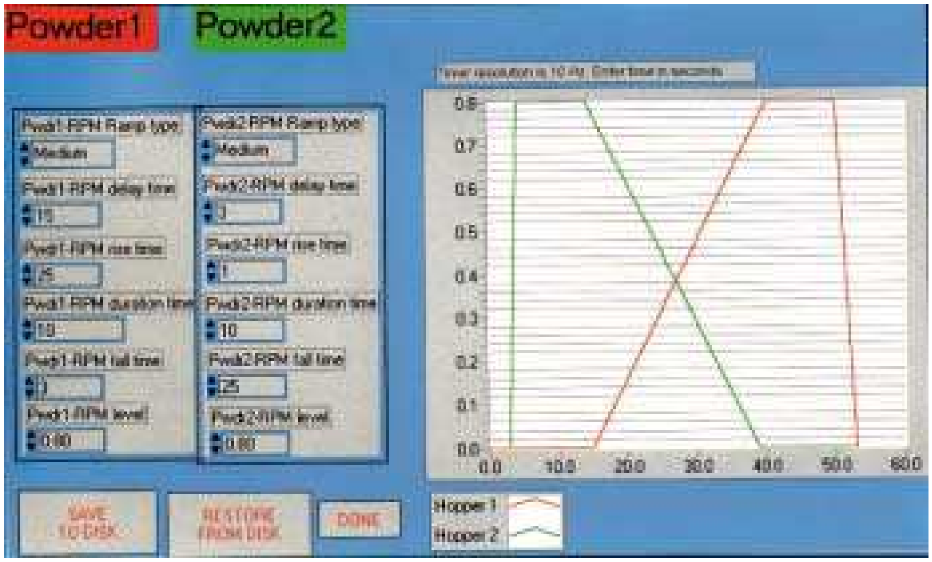

Figure 4. Computer based control system used to control the powder hopper dispensing rate for producing the $MoSi_2$-Al_2O_3 graded structures. Powder 1 is $MoSi_2$ and Powder 2 is Al_2O_3

3. Results and Discussion

Figure 5 shows the cross-sections of laminate $MoSi_2$-Al_2O_3 tubes that were fabricated by plasma spraying alternate layers of $MoSi_2$ and Al_2O_3 onto a graphite tube mandrel (the graphite mandrel is subsequently removed by oxidation). The composition of these composite tubes is 50-50 vol.% $MoSi_2$-Al_2O_3 ($MoSi_2$ is the dark phase and Al_2O_3 is the light phase). Tubes with three different layer thicknesses of 0.7 mm, 0.18 mm, and 0.07 mm were fabricated. The fabricated tubes were approximately 300 mm in length. Shown in Figure 6 are the room temperature four-point bend strengths of these composites. Composite strengths were in the range of 85-115 MPa and were observed to increase with decreasing layer thickness. Such a trend is consistent with a decrease in the fracture-initiating defect size as the layer thickness is reduced. Concave down and up refers to the curvature of the laminate layers in relation to the tensile surface of the bend specimen. There was essentially no effect of this curvature on bend strength.

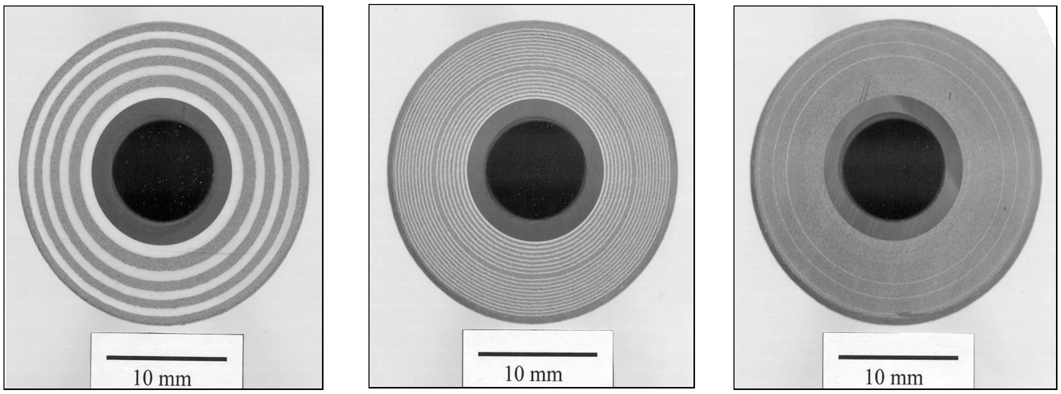

layer thickness 0.7 mm　layer thickness 0.17 mm　layer thickness 0.07 mm

Figure 5. Fifty vol.% $MoSi_2$-50 vol.% Al_2O_3 laminate composites produced by plasma spray-forming.

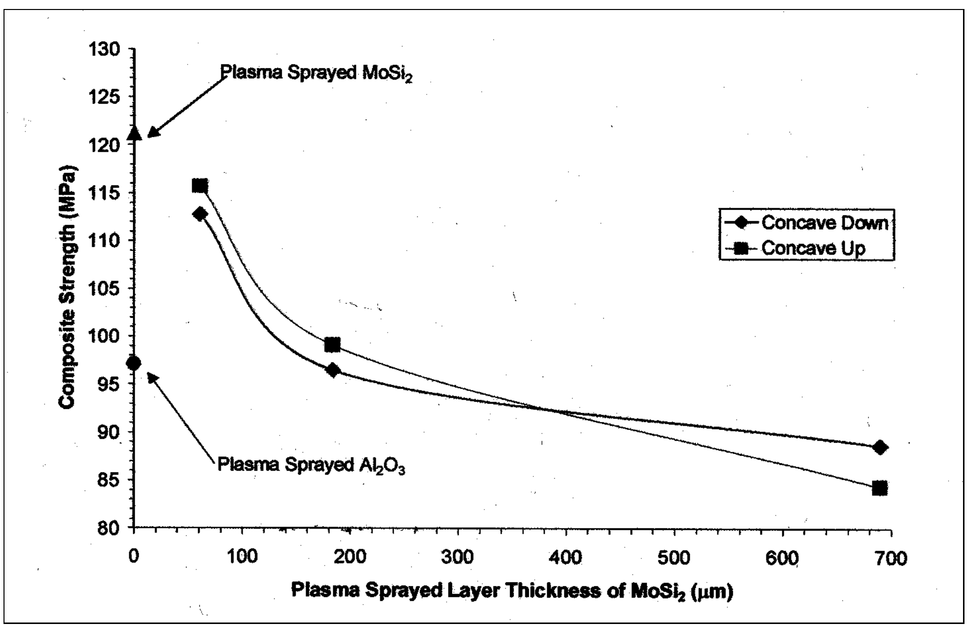

Figure 6. Variation in the bend strength of the layered composites as a function of layer thickness.

Figure 7 shows the cross-sections of functionally graded $MoSi_2$-Al_2O_3 tubes fabricated by plasma spray-forming. Al_2O_3 is the light phase. Both continuously graded and layered graded tubes were fabricated. Room temperature C-ring strength distribution for these functionally graded tubes are shown in Figure 8. Strengths were observed to be in the range of 55-80 MPa. The continuously graded material exhibited both a higher strength and a reduced strength scatter, as compared to the layered and graded material.

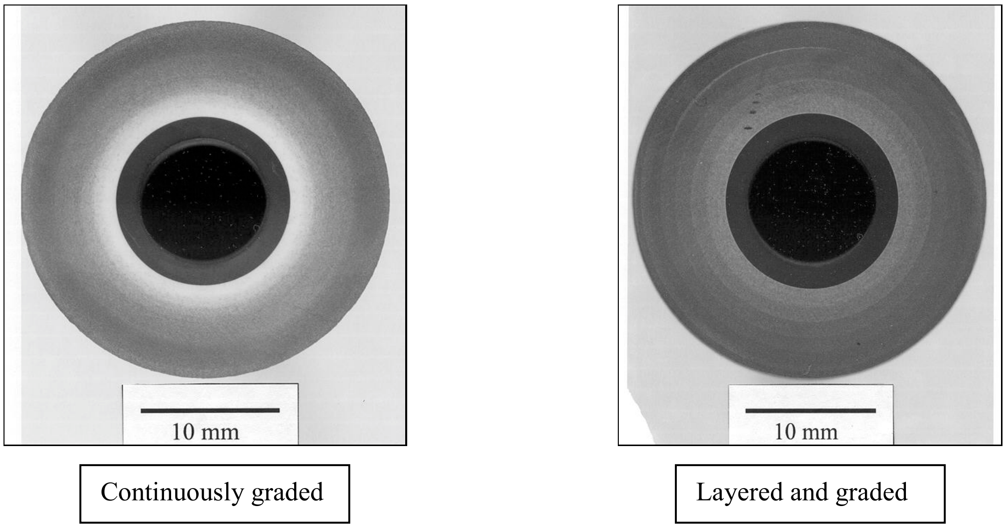

Figure 7. Continuously graded and layered graded $MoSi_2$-Al_2O_3 composites. Al_2O_3 is the light phase and $MoSi_2$ is the dark phase.

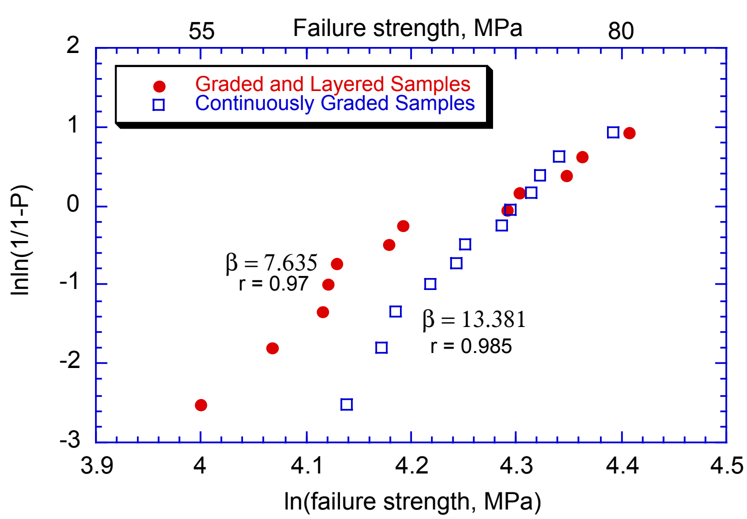

Figure 8. Weibull probability failure plots obtained from the C-ring tests performed on the graded samples.

Although the strength of the graded composite samples was not significantly improved over monolithic $MoSi_2$, the fracture energy of these composite samples was significantly higher than that of monolithic $MoSi_2$. Representative load-displacement curves for the composite samples are compared to those for the monolithic materials in Figure 9. The average fracture energy values calculated from the area under the load-displacement curves (using the entire specimen fracture area) gave the following values:

monolithic Al_2O_3 - 285.3 J/m^2
monolithic $MoSi_2$ - 496.3 J/m^2
continuously graded $MoSi_2/Al_2O_3$ composite - 955 J/m^2
layered and graded $MoSi_2/Al_2O_3$ composite – 766.3 J/m^2

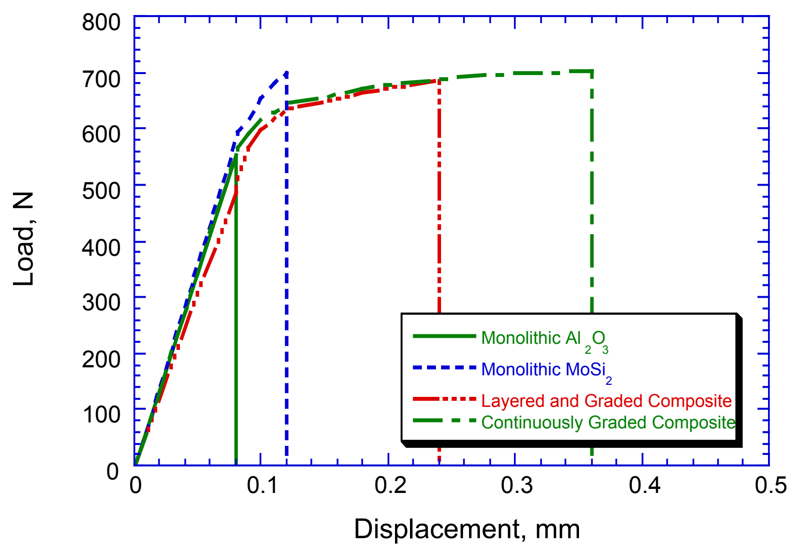

Figure 9. Load-displacement plots obtained from the C-ring tests performed on the graded samples.

This improvement in fracture energy (an indirect measure of fracture toughness) is a result of microscopic crack deflection resulting in a tortuous crack path through the material, and was verified through scanning electron microscopy and surface roughness measurements.

4. Concluding Remarks

We have demonstrated the use of conventional plasma spraying equipment in manufacturing $MoSi_2$-Al_2O_3 functionally graded and layered composites. The mechanical performance of these materials is superior to that of the monolithic materials. This was verified through C-ring and bend tests. Although the molten glass corrosion behavior of the composite materials is acceptable below and above the glass line, the corrosion rate at the glass line is higher than desirable. Processing of $MoSi_2$ based composites coatings is ongoing and it will be determined if these tailored microstructures will reduce the glass-line corrosion.

Acknowledgements

This research has been supported by the U.S. Department of Energy, Office of Industrial Technologies, Glass Industry Program. The authors would like to acknowledge the technical support given by Richard Hoover, Maria Peters, and Daniel Mendoza at Los Alamos National Laboratory.

References

1. Y.S. Park, D.P. Butt, R. Castro, J. Petrovic, W. Johnson, *Materials Science and Engineering*, **A261**, 278-283 (1999).
2. J.J Petrovic., *Materials Research Society Bulletin*, **XVIII 35**, (1993).
3. J.J Petrovic, and A.K. Vasudevan, *Materials Research Society Symposium Proceedings*, 322, 3 (1994).
4. R.G. Castro, H. Kung, K.J. Hollis and A.H. Bartlett, *15th International Thermal Spray Conference*, Nice, France May 25-29, 1199-1204 (1998).
5. A.H. Bartlett, R.G. Castro, D.P. Butt, H. Kung, Z. Zurecki and J.J. Petrovic, *Industrial Heating*, January 33-36 (1996).